

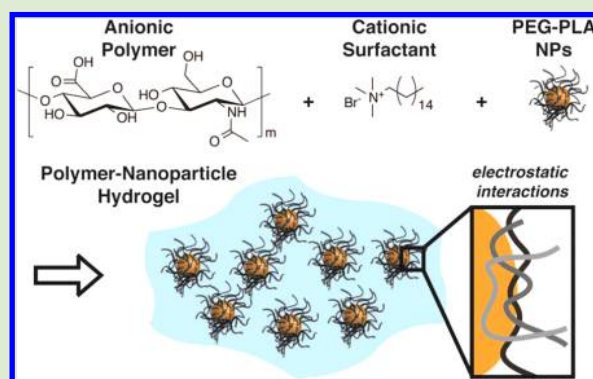
# Exploiting Electrostatic Interactions in Polymer–Nanoparticle Hydrogels

Eric A. Appel, Mark W. Tibbitt, Jessica M. Greer, Owen S. Fenton, Klaus Kreuels, Daniel G. Anderson, and Robert Langer\*

David H. Koch Institute for Integrative Cancer Research, Department of Chemical Engineering, and Division of Health Science and Technology, Massachusetts Institute of Technology, 77 Massachusetts Avenue, Cambridge, Massachusetts 02139, United States

## S Supporting Information

**ABSTRACT:** Shear-thinning injectable hydrogels exploit dynamic noncovalent cross-links to flow upon applied stress and rapidly self-heal once the stress is relaxed. These materials continue to gather interest as they afford minimally invasive deployment in the body for a variety of biomedical applications. Here, we present rationally engineered polymer–nanoparticle (PNP) interactions based on electrostatic forces for the fabrication of self-assembled hydrogels with shear-thinning and self-healing properties. The selective adsorption of negatively charged biopolymers, including hyaluronic acid (HA) and carboxymethylcellulose (CBMC), to biodegradable nanoparticles comprising poly(ethylene glycol)-*b*-poly(lactic acid) (PEG-*b*-PLA) is enhanced with a positively charged surfactant, cetyltrimethylammonium bromide (CTAB). We demonstrate that, in this manner, electrostatic interactions can be leveraged to fabricate PNP hydrogels and characterize the viscoelastic properties of the gels imparted by CBMC and HA. This work introduces PNP hydrogels that use common biopolymers without the need for chemical modification, yielding extremely facile preparation and processing, which when coupled with the tunability of their properties are distinguishing features for many important biomedical and industrial applications.



Shear-thinning injectable hydrogels are an important class of soft matter, finding broad applicability in biomedicine, including tissue engineering and controlled drug delivery.<sup>1</sup> Recently in polymer science, rationally designed noncovalent interactions operating in aqueous media, and providing reversible control over the self-assembly process, have yielded new types of shear-thinning hydrogels.<sup>2</sup> These materials exhibit many unique and useful properties, including externally tunable strength, moldability, low-energy synthesis/processing, and self-healing.<sup>2</sup> Several classes of these materials have been developed and evaluated in various applications and exploit many different types of interactions for noncovalent cross-linking including host–guest interactions,<sup>3–11</sup> ionic interactions,<sup>12–14</sup> metal–ligand coordination,<sup>15</sup> rationally designed biopolymer self-assembly,<sup>16–23</sup> as well as natural biopolymer cross-linking.<sup>24,25</sup> Moreover, shear-responsive colloidal hydrogels comprising mixtures of positively and negatively polymeric nanoparticles self-assembling with favorable electrostatic interactions have been developed in various ways.<sup>26–28</sup>

We have reported a new class of shear-thinning and injectable polymer–nanoparticle (PNP) hydrogels<sup>29</sup> that exploit dynamic and multivalent interactions between polymers and nanoparticles.<sup>30</sup> PNP gels form rapidly upon mixing of aqueous solutions of appropriately paired polymers and nanoparticles, such that the polymers selectively adsorb to

the nanoparticles and exhibit dramatic shear-thinning and rapid self-healing. For example, PNP gels have been fabricated from hydrophobically modified hydroxypropylmethylcellulose (HPMC- $C_x$ )<sup>31</sup> and nanoparticles composed of poly(ethylene glycol)-*block*-poly(lactic acid) (PEG-*b*-PLA) as a platform for injectable drug delivery.<sup>29</sup> Moreover, a robust physical model for efficient cross-linking in PNP hydrogels highlights three important parameters: (i) affinity between nanoparticles and polymers where the free energy gain is greater than thermal energy ( $\epsilon > k_B T$ ), (ii) the number of cross-linking interactions ( $n$ ), and (iii) nanoparticle size relative to the persistence length of the polymers ( $D_H < l_p$ ). The strength of the materials ( $G$ ), therefore, can be related to the number of polymer–nanoparticle interactions per unit volume ( $n$ ) and the energy associated with each interaction ( $\alpha k_B T$ ) using theoretical tools analogous to those developed for covalent hydrogels:  $G \approx n \alpha k_B T$ .<sup>32</sup> Furthermore, owing to the hierarchical structure of the PNP hydrogels, molecular cargo can be entrapped and delivered in a controlled manner, independently by either Fickian diffusion (hydrophilic) or erosion (hydrophobic), thus affording differential release of multiple compounds from a

Received: June 21, 2015

Accepted: July 1, 2015

single material, which has been validated both *in vitro* and *in vivo*.<sup>29</sup>

Herein we prepare PNP-based materials utilizing two biopolymers that have found broad utility as biomaterials (Figure 1): carboxymethylcellulose (CBMC;  $M_w \sim 700$  kDa)

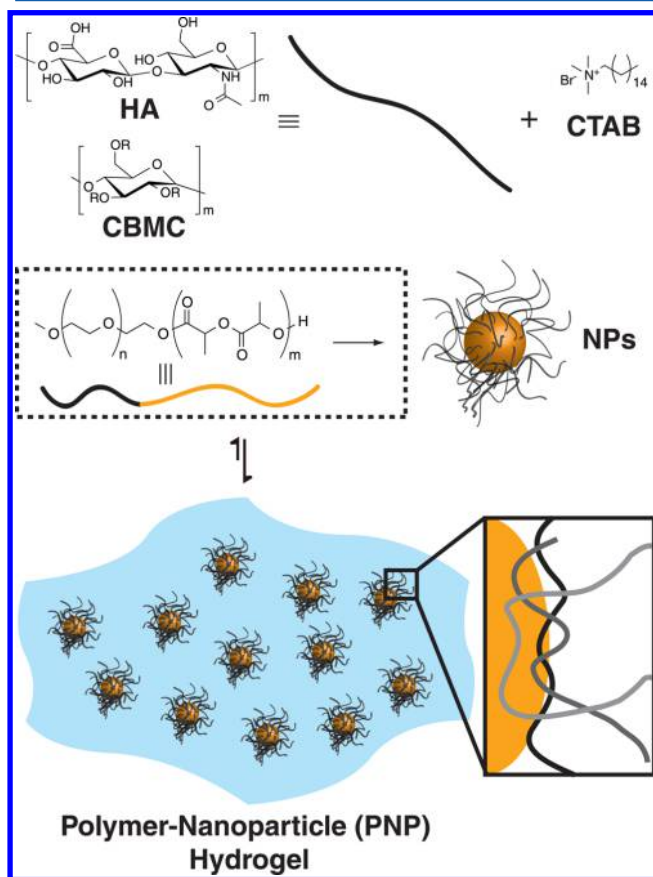


Figure 1. Schematic representation of the preparation of polymer-nanoparticle (PNP) hydrogels using electrostatic interactions. (a) Polymers negatively charged at physiological pH, i.e., hyaluronic acid (HA) or carboxymethylcellulose (CBMC;  $R = -CH_2-COOH$ ), can be noncovalently modified via addition of cetyltrimethylammonium bromide (CTAB). (b) Amphiphilic poly(ethylene glycol)-*b*-poly(lactic acid) (PEG-*b*-PLA) polymers can be nanoprecipitated from water to form biodegradable nanoparticles (NPs). (c) PNP hydrogels are prepared by simply mixing PEG-*b*-PLA NPs with HA/CTAB or CBMC/CTAB.

and hyaluronic acid (HA; bacterial glycosaminoglycan polysaccharide from *Streptococcus equi*). CBMC has been used extensively in the past as a viscosity modifier in food, pharmaceuticals, and cosmetics, as well as a biomaterial building block in various biomedical applications, including drug delivery and tissue engineering, demonstrating a high level of biocompatibility and low toxicity.<sup>33</sup> HA was selected for its many past uses in biological materials,<sup>19</sup> its capability to be easily chemically modified as needed,<sup>34</sup> as well as the high level of biocompatibility it demonstrates, being that it is found in certain places in the body, such as the eye and the extra cellular matrix.<sup>35</sup> Moreover, Burdick and co-workers have recently prepared shear-thinning injectable hydrogels utilizing cyclodextrin-based supramolecular cross-linking of HA.<sup>3,36</sup> As stated above, one of the important factors in determining the mechanical properties of PNP hydrogels is the energetic favorability of the interactions between the NP and the

polymer. As both of these biopolymers are anionically charged at physiological pH, we hypothesized it would be possible to exploit electrostatic interactions to facilitate polymer-nanoparticle interactions leading to hydrogel formation. We therefore decided to investigate if the addition of a cationic surfactant molecule, cetyltrimethylammonium bromide (CTAB), would impart sufficient interaction strength between the anionic biopolymers (via electrostatic interactions) and the core-shell nanoparticles (via hydrophobic interactions).

First, we synthesized PEG<sub>5k</sub>-*b*-PLA<sub>20k</sub> utilizing organocatalytic ring-opening polymerization techniques according to literature procedures.<sup>37</sup> This polymer was chosen as it has been utilized previously in the preparation of PEG-*b*-PLA NPs in a size regime amenable to PNP hydrogel formation ( $D_H \sim 100$  nm).<sup>29</sup> Following preparation of PEG-*b*-PLA NPs by nanoprecipitation according to literature procedures,<sup>38</sup> the NPs were concentrated for use in PNP hydrogel preparation ( $[NPs] = 15\%$ ). We then prepared an aqueous solution of CBMC (3%) and CTAB (1.5%). The solutions of CBMC/CTAB and PEG-*b*-PLA NPs were then mixed vigorously to a final concentration by weight percent of CBMC:NP:CTAB (1:10:0.5), based on previous formulations.<sup>29</sup> Figure 2 demonstrates that the

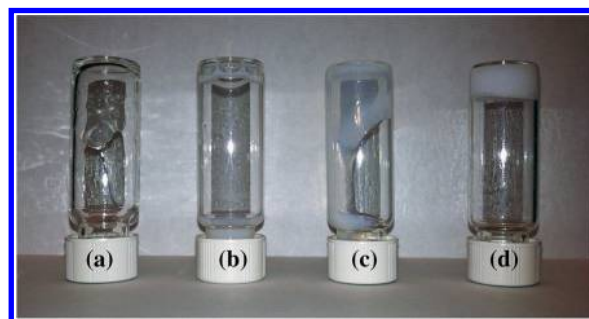
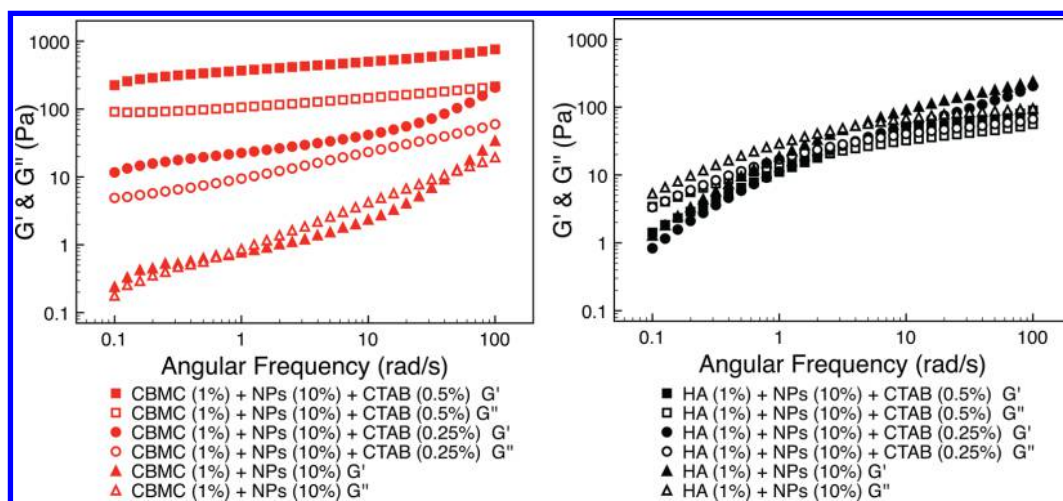


Figure 2. Inverted vial test of PNP hydrogels exploiting electrostatic interactions between nonfunctionalized, anionic polymers and NPs in the presence of cetyltrimethylammonium bromide (CTAB): (a) CBMC (1%), (b) NPs (10%), (c) CBMC (1%) + NPs (10%), and (d) CBMC (1%) + NPs (10%) + CTAB (0.25%).

interaction between the CBMC polymer and the NPs alone is not sufficiently strong to induce hydrogel formation, and hydrogels are formed exclusively when all three components are present. In order to study the effects of the CTAB on hydrogel formation, we repeated the process across a series of CTAB concentrations, where we observed that above a maximum CTAB concentration of 0.5% the anionic polymers precipitated from solution.

With convincing qualitative data in hand demonstrating the ability of the enhancement of native PNP interactions with electrostatic interactions via addition of a charged surfactant, we then sought to quantitatively study the mechanical properties of these materials. We prepared a series of hydrogel materials with CBMC and HA polymers for rheological characterization. Frequency-dependent rheological characterization of these materials, performed in the linear viscoelastic region, is shown in Figure 3. The frequency dependence of the storage and loss oscillatory shear moduli ( $G'$  and  $G''$ , respectively), clearly identifies hydrogel-like behavior in the CBMC-based materials (Figure 3a) exclusively in the presence of CTAB, as the two are linear and parallel and  $G'$  is dominant across the whole range of frequencies observed. In general, these hydrogels are soft ( $G' \approx 0.5$  kPa at 0.5% loading of CTAB)



**Figure 3.** Frequency-dependent oscillatory rheological characterization ( $\gamma = 2\%$ ) of PNP hydrogels comprising (a) CBMC and (b) HA.

yet are highly elastic ( $\tan \delta = G''/G' \approx 0.2$ ). Moreover, the mechanical properties of the material can be tuned over several orders of magnitude simply through alteration of the formulation. Again, the formation of robust hydrogels is specific to the combination of all three components: CBMC, NPs, and CTAB (Figure S1, Supporting Information).

In contrast, the material properties of the HA-based materials (Figure 3b) are independent of the concentration of CTAB, where hydrogels are formed with only HA and NPs. These materials exhibit viscoelastic behavior, where the crossover of  $G'$  and  $G''$  is observed at frequencies around 2 rad/s. Presumably, the native PNP interaction strength between HA and the NPs is sufficiently strong to yield hydrogel formation. Moreover, zeta-potential measurements of HA ( $-7.8 \pm 1.2$  mV) identify that there is significantly lower negative charge density on HA when compared with CBMC ( $-29.7 \pm 2.0$  mV), corroborating our previous observations where the mechanical properties of CBMC-based materials are highly dependent on CTAB concentration. These observations support our physical model, whereby hydrogel strength is proportional to the free energy gain from the PNP interactions ( $G \propto \epsilon$ ), which in the case of CBMC are enhanced by electrostatic interactions with the CTAB-modified NPs. Furthermore, the viscoelastic rheological behavior of the HA-based materials formed from native PNP interactions likely arises from the smaller persistence length of HA relative to CBMC, which is perhaps also related to the lower anionic charge density along the polymer chain.

To investigate further the role of electrostatic interactions in PNP hydrogels, we prepared materials with CBMC at increased ionic strength utilizing addition of low (1 mM) and high (100 mM) concentrations of sodium chloride (NaCl; Figure S2, Supporting Information). Increased ionic strength can act to shield electrostatic interactions, which led to a 5-fold decrease in the storage modulus of CBMC-based PNP hydrogels. These data further highlight the key role of electrostatic interactions in the preparation of robust PNP hydrogels from anionic biopolymers via addition of a cationic surfactant.

We then sought to explore the ability to prepare mixed-polymer systems with both HA and CBMC to demonstrate the general nature of the noncovalent interactions and their amenability to combinatorial mixing, which may allow for synergism between the mechanical stability of CBMC with the enhanced biodegradability of HA. Figure 4 demonstrates that

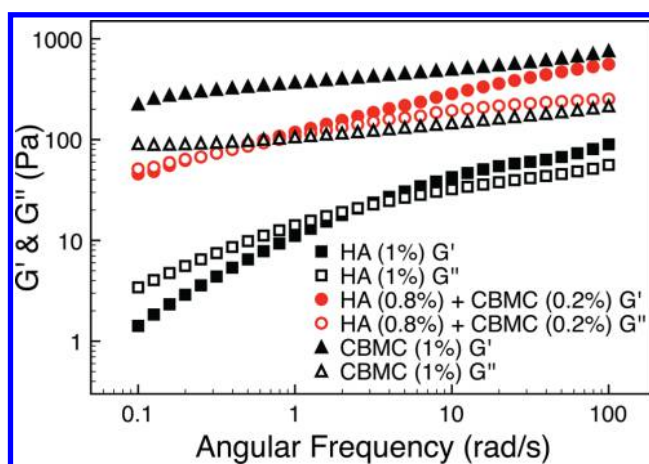


**Figure 4.** Frequency-dependent oscillatory rheological characterization ( $\gamma = 2\%$ ) of PNP hydrogels prepared from HA, CBMC, NPs (10%), and CTAB (0.5%). The modular electrostatic interactions responsible for cross-linking allow for facile alteration of mechanical properties via modulation of the formulation.

materials prepared from HA (0.8%), CBMC (0.2%), CTAB (0.5%), and NPs (10%) exhibit intermediate properties between those of materials prepared with CBMC or HA alone. Thus, materials composed primarily of HA can be prepared with significantly enhanced mechanical properties (i.e.,  $>1$  order of magnitude increase in  $G'$ ) by simple addition of a small proportion of CBMC into the formulation.

Additionally, strain-dependent oscillatory rheology (Figure S3, Supporting Information) of the materials formed from PEG-PLA NPs (10%), HA or CBMC (1%), and CTAB (0.25 or 0.5%) demonstrates an extremely broad linear viscoelastic region, indicating that these materials have an extensive processing regime. The relative loadings of CTAB and the various biopolymers used can produce materials with a large range of mechanical properties. It is only when CBMC is used that a deviation from linear viscoelasticity is observed as a breakdown of the hydrogel structure at strain amplitudes above 10% yields a large decrease in oscillatory shear modulus resulting from network rupture. This property is typically indicative of highly dynamic cross-linking,<sup>5</sup> which allows for rapid (relative to the experimental frequency) rearrangement of the network in response to applied strain.



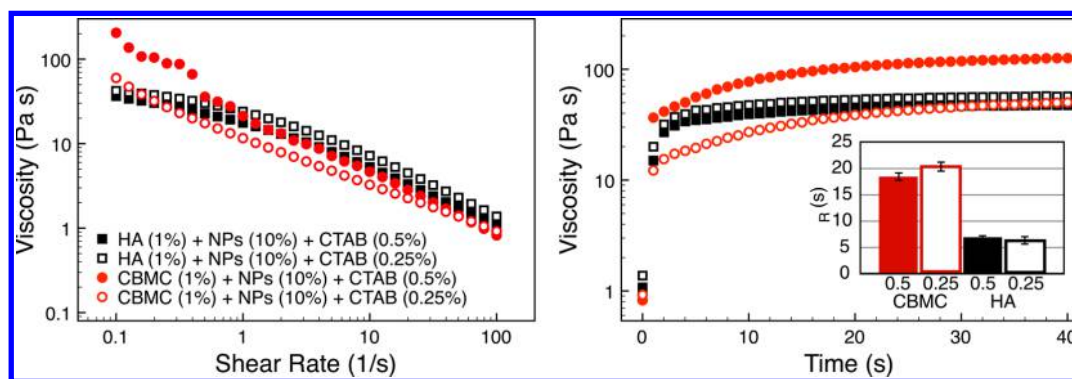


**Figure 5.** Flow rheological characterization of PNP hydrogels: (a) steady-shear measurements and (b) step-rate time-sweep measurements displaying recovery of hydrogel structure at low shear rate ( $\dot{\gamma} = 0.1 \text{ s}^{-1}$ ) following high-magnitude deformation ( $\dot{\gamma} = 100 \text{ s}^{-1}$ ). Fitting of viscosity recovery following to a single-stage association model ( $R^2 > 0.98$ ) yields a characteristic time ( $\tau_R$ ) for recovery of the hydrogel structure (inset;  $n = 3$ ).

According to steady shear rheological measurements (Figure 5a and Figure S4, Supporting Information), all of the hydrogels prepared herein are shear-thinning ( $\eta = 100 \rightarrow 1 \text{ Pa s}$  from  $\dot{\gamma} = 0.1 \rightarrow 100 \text{ s}^{-1}$ ), which is consistent with previous observations for supramolecular cross-linked materials.<sup>5</sup> The steady shear measurements of the CBMC-based materials follow a power law relationship, similar to other supramolecular cross-linked materials prepared from cellulose derivatives,<sup>4</sup> with high-shear viscosities sufficiently low to make them amenable to injection.<sup>19,21,22,29,36</sup> Interestingly, these materials also exhibit a nontrivial difference in viscosity in the low-shear regime ( $\dot{\gamma} = 0.1 \text{ s}^{-1}$ ), whereby higher CTAB loading corresponds to a roughly 2.5 $\times$  increase in viscosity, while the viscosity of these materials in the high-shear regime ( $\dot{\gamma} = 100 \text{ s}^{-1}$ ) is independent of the CTAB concentration. These observations support the hypothesis that the noncovalent interactions responsible for cross-linking between polymer chains and NPs are disrupted by the application of physical stress to the materials. Again, HA-based materials exhibit a slightly different rheological behavior than the CBMC-based materials and no significant dependence on CTAB concentration.

Step rate measurements were performed to investigate the recovery of hydrogel material properties following deformation at high shear rates (Figure 5b). A high magnitude shear rate ( $\dot{\gamma} = 100 \text{ s}^{-1}$ ) was applied to break down the hydrogel structure, followed by a low magnitude shear rate ( $\dot{\gamma} = 0.1 \text{ s}^{-1}$ ) in order to monitor the rate and extent of recovery of bulk material properties. Figure 5b clearly demonstrates the exceptionally fast and complete recovery of viscosity after destruction of the gel structure in a matter of a few seconds. Previous materials exhibiting such rapid self healing have highlighted a strong correlation with rapid association kinetics of the supramolecular interactions.<sup>5,7,9</sup> These data were fit with a single-stage association model, and a characteristic time for recovery ( $\tau_R$ ) for each material is shown in the inset. The rate of material property recovery is polymer dependent, where the HA-based materials exhibit significantly faster recovery than the CBMC-based materials, likely on account of the greater chain flexibility. Moreover, the HA-based materials, similar to their other rheological behavior, do not exhibit significantly different recovery rates. In contrast, the CBMC-based materials do exhibit slight differences, where more rapid recovery is observed in materials with a higher loading of CTAB, and thus a stronger association between the CBMC polymers and the NPs.

In summary, self-assembled PNP hydrogels formulated from commercially available biopolymers and biodegradable core-shell nanoparticles of PEG-*b*-PLA have been prepared, exhibiting highly tunable mechanical properties and broadening the scope of the PNP hydrogel platform. These materials are readily processed, and the simplicity of their preparation, their availability from inexpensive biocompatible and biodegradable resources, as well as the broad tunability of their mechanical properties are distinguishing for many important biomedical applications. The diversity of both synthetic and natural materials and the additional flexibility of utilizing mixtures of biopolymers as well as surfactant concentration (as well as the opportunity for using other surfactants) provide a useful tool with which to tune properties.

## ■ ASSOCIATED CONTENT

### 📄 Supporting Information

Instrumentation and materials, general synthesis of PEG-*b*-PLA block copolymers, general preparation of self-assembled hydrogels, in vivo administration, and supplementary figures. The Supporting Information is available free of charge on the ACS Publications website at DOI: 10.1021/acsmacrolett.5b00416.

## ■ AUTHOR INFORMATION

### Corresponding Author

\*E-mail: rlander@mit.edu.

### Notes

The authors declare no competing financial interest.

## ■ ACKNOWLEDGMENTS

E.A.A. is extremely grateful for financial support through a Wellcome Trust-MIT Postdoctoral Fellowship and a Margaret A. Cunningham Fellowship Award. M.W.T. is grateful for financial support through a fellowship from the Misrock Foundation. The work is supported in part by NIH-R01 DE016516.

## ■ REFERENCES

- (1) Guvendiren, M.; Lu, H. D.; Burdick, J. A. *Soft Matter* **2012**, *8*, 260–272.
- (2) Appel, E. A.; del Barrio, J.; Loh, X. J.; Scherman, O. A. *Chem. Soc. Rev.* **2012**, *41*, 6195–6214.
- (3) Rodell, C. B.; Kaminski, A.; Burdick, J. A. *Biomacromolecules* **2013**, *14*, 4125–4134.

- (4) Appel, E. A.; Loh, X. J.; Jones, S. T.; Biedermann, F.; Dreiss, C. A.; Scherman, O. A. *J. Am. Chem. Soc.* **2012**, *134*, 11767–11773.
- (5) Appel, E. A.; Biedermann, F.; Rauwald, U.; Jones, S. T.; Zayed, J. M.; Scherman, O. A. *J. Am. Chem. Soc.* **2010**, *132*, 14251–14260.
- (6) Appel, E. A.; Loh, X. J.; Jones, S. T.; Dreiss, C. A.; Scherman, O. A. *Biomaterials* **2012**, *33*, 4646–4652.
- (7) Mckee, J.; Appel, E. A.; Seitsonen, J.; Kontturi, E.; Scherman, O. A.; Ikkala, O. *Adv. Funct. Mater.* **2014**, *24*, 2706–2713.
- (8) Rowland, M. J.; Appel, E. A.; Coulston, R. J.; Scherman, O. A. *J. Mater. Chem. B* **2013**, *1*, 2904–2910.
- (9) Appel, E. A.; Koutsioubas, A.; Toprakcioglu, C.; Scherman, O. A. *Angew. Chem., Int. Ed.* **2014**, *53*, 10038–10043.
- (10) Appel, E. A.; Forster, R. A.; Rowland, M. J.; Scherman, O. A. *Biomaterials* **2014**, *35*, 9897–9903.
- (11) Park, K. M.; Yang, J.-A.; Jung, H.; Yeom, J.; Park, J. S.; Park, K.-H.; Hoffman, A. S.; Hahn, S. K.; Kim, K. *ACS Nano* **2012**, *6*, 2960–2968.
- (12) Hunt, J. N.; Feldman, K. E.; Lynd, N. A.; Deek, J.; Campos, L. M.; Spruell, J. M.; Hernandez, B. M.; Kramer, E. J.; Hawker, C. J. *Adv. Mater.* **2011**, *23*, 2327–2331.
- (13) Wang, Q.; Mynar, J. L.; Yoshida, M.; Lee, E.; Lee, M.; Okuro, K.; Kinbara, K.; Aida, T. *Nature* **2010**, *463*, 339–343.
- (14) Mynar, J. L.; Aida, T. *Nature* **2008**, *451*, 895–896.
- (15) Holten-Andersen, N.; Harrington, M. J.; Birkedal, H.; Lee, B. P.; Messersmith, P. B.; Lee, K. Y. C.; Waite, J. H. *Proc. Natl. Acad. Sci. U. S. A.* **2011**, *108*, 2651–2655.
- (16) Petka, W. A.; Harden, J. L.; McGrath, K. P.; Wirtz, D.; Tirrell, D. A. *Science* **1998**, *281*, 389–392.
- (17) Olsen, B. D.; Kornfield, J. A.; Tirrell, D. A. *Macromolecules* **2010**, *43*, 9094–9099.
- (18) Shen, W.; Zhang, K. C.; Kornfield, J. A.; Tirrell, D. A. *Nat. Mater.* **2006**, *5*, 153–158.
- (19) Lu, H. D.; Soranno, D. E.; Rodell, C. B.; Kim, I. L.; Burdick, J. A. *Adv. Healthcare Mater.* **2013**, *2*, 1028–1036.
- (20) Lu, H. D.; Charati, M. B.; Kim, I. L.; Burdick, J. A. *Biomaterials* **2012**, *33*, 2145–2153.
- (21) Wong Po Foo, C. T. S.; Lee, J. S.; Mulyasmita, W.; Parisi-Amon, A.; Heilshorn, S. C. *Proc. Natl. Acad. Sci. U. S. A.* **2009**, *106*, 22067–22072.
- (22) Parisi-Amon, A.; Mulyasmita, W.; Chung, C.; Heilshorn, S. C. *Adv. Healthcare Mater.* **2013**, *2*, 428–432.
- (23) Cai, L.; Dewi, R. E.; Heilshorn, S. C. *Adv. Funct. Mater.* **2015**, *25*, 1344.
- (24) Ta, H. T.; Dass, C. R.; Dunstan, D. E. *J. Controlled Release* **2008**, *126*, 205–216.
- (25) Augst, A. D.; Kong, H. J.; Mooney, D. J. *Macromol. Biosci.* **2006**, *6*, 623–633.
- (26) Gu, Z.; Aimetti, A. A.; Wang, Q.; Dang, T. T.; Zhang, Y.; Veisoh, O.; Cheng, H.; Langer, R. S.; Anderson, D. G. *ACS Nano* **2013**, *7*, 4194–4201.
- (27) Wang, Q.; Wang, L.; Detamore, M. S.; Berkland, C. *Adv. Mater.* **2008**, *20*, 236–239.
- (28) Wang, Q.; Wang, J.; Lu, Q.; Detamore, M. S.; Berkland, C. *Biomaterials* **2010**, *31*, 4980–4986.
- (29) Appel, E. A.; Tibbitt, M. W.; Webber, M. J.; Mattix, B. A.; Veisoh, O.; Langer, R. *Nat. Commun.* **2014**, *6*, 6295.
- (30) Rose, S.; PrevotEAU, A.; Elzière, P.; Hourdet, D.; Marcellan, A.; Leibler, L. *Nature* **2014**, *505*, 382–385.
- (31) Chiellini, E.; Sunamoto, J.; Migliaresi, C.; Ottenbrite, R. M.; Cohn, D., Eds. *Biomedical Polymers and Polymer Therapeutics*; Kluwer Academic/Plenum Publishers: Norwell, MA, 2001.
- (32) Rubinstein, M.; Colby, R. H. *Polymer Physics*; Oxford University Press: New York, 2003.
- (33) Heinze, T.; Koschella, A. *Macromol. Symp.* **2005**, *223*, 13–40.
- (34) Ifkovits, J. L.; Burdick, J. A. *Tissue Eng.* **2007**, *13*, 2369–2385.
- (35) Burdick, J. A.; Prestwich, G. D. *Adv. Mater.* **2011**, *23*, H41–H56.
- (36) Rodell, C. B.; MacArthur, J. W.; Dorsey, S. M.; Wade, R. J.; Wang, L. L.; Woo, Y. J.; Burdick, J. A. *Adv. Funct. Mater.* **2015**, *25*, 636–644.
- (37) Lohmeijer, B.; Pratt, R.; Leibfarth, F.; Logan, J.; Long, D.; Dove, A.; Nederberg, F.; Choi, J.; Wade, C.; Waymouth, R.; Hedrick, J. L. *Macromolecules* **2006**, *39*, 8574–8583.
- (38) Cheng, J.; Teply, B.; Sherifi, I.; Sung, J.; Luther, G.; Gu, F.; Levy-Nissenbaum, E.; Radovic-Moreno, A.; Langer, R.; Farokhzad, O. *Biomaterials* **2007**, *28*, 869–876.